Do Wind Turbines Amplify the Effects of Lightning Strikes? A Full-Maxwell Modelling Approach

Riccardo Torchio, Martino Nicora, *Member, IEEE*, Daniele Mestriner, *Member, IEEE*, Massimo Brignone, *Member, IEEE*, Renato Procopio, *Senior Member, IEEE*, Piergiorgio Alotto, *Senior Member, IEEE*, and Marcos Rubinstein, *Fellow, IEEE*

***Abstract*—Wind turbines (WTs) can be seriously damaged by lightning strikes and they can be struck by a significant number of flashes. This should be taken into account when the WT lightning protection system is designed. Moreover, WTs represent a path for the lightning current that can modify the well-known effects of the lightning discharge in terms of radiated electromagnetic fields, which are a source of damage and interference for nearby structures and systems. In this paper, a WT struck by a lightning discharge is analyzed with a full-wave modelling approach, taking into account the details of the WT and its interactions with the lightning channel. The effects of first and subsequent return strokes are analyzed as well as that of the rotation angle of the struck blade. Results show that the lightning current along the WT is mainly affected by the ground reflection and by the reflection between the struck blade and the channel. The computed electromagnetic fields show that, for subsequent return strokes, the presence of a WT almost doubles their magnitude with respect to a lightning striking the ground. Such enhancement is emphasized when the inclined struck blade is considered.**

***Index Terms*—Lightning, wind turbines, renewable, lightning at tall structures, return stroke current, lightning electromagnetic pulse.**

I. Introduction

WIND energy has progressively become one of the fastest developing and widely used power sources in many countries around the world. The estimated electricity production from wind power in the European Union is 426 TWh in 2019, supplying 14% of the total demand; the installed power in the European Union reached 167.6 GW in 2019, with an increase of 10 GW of capacity, compared to just over 8.7 GW in 2018 [1].

The height of WTs and their location, often in mountainous regions, makes them very exposed to the lightning hazard [2], [3]. Tall WTs attract downward flashes, but they initiate an appreciable number of upward flashes as well [4]. The proportion of initiated upward flashes depends on different factors such as the structure height and the local terrain elevation [5], [6]. The rotation of the blades may also trigger lightning [7]–[9]. Field observations revealed that a significant number of direct lightning strikes are experienced by WTs during their lifetime [10], [11]. Lightning attachment to WTs may cause severe damages and high repair costs, considering materials, labor, insurance claims and downtime [12]–[15]. Lightning hazard is expected to increase with the development of technology, since new generation WTs are characterized by greater heights, ever smaller and more vulnerable electronics and poor-conductivity carbon-fiber composite reinforcements in the rotor blades [7].

WT lightning protection is addressed in detail in the IEC 61400-24 standard [16]. Typically, the lightning attachment occurs at the air-termination system installed on rotor blades; then, through the metal conductor that runs inside the rotor blade, the lightning current is transferred into the hub, the nacelle and it then flows along the WT tower and dissipates into the ground through the earth-termination system.

The aim of this paper is to perform an accurate analysis of the WT transient response to direct lightning strikes in order to get the spatial-temporal current distribution along the WT and in the lightning channel. The obtained current waveforms are used to compute the radiated ElectroMagnetic (EM) fields from which one can calculate the over-voltages induced on nearby electrical systems (power distribution lines, in particular) and assess the effects of the presence of the WT. Actually, it has been found that the presence of a tall strike object may significantly increase – up to a factor of about three – the electric and magnetic field peaks and their derivatives at a distance exceeding its height (e.g., [17], [18]).

Due to their high amplitude and steepness, lightning currents may cause extremely high potential differences inside the WT, giving rise to dangerous over-voltages on electrical and electronic components [19]. The transient analysis presented in this paper may be applied to improve the design of measures against undesirable sparking (separation distances between conductors, insulation of conductors, equipotential bonding, surge protection devices).

The paper is organized as follows. Section II discusses the problem of modelling lightning-return strokes to tall objects, with particular focus on WTs. The adopted model is completely described in Section III (geometries and materials, numerical method, challenges and assumptions). Section

R. Torchio and P. Alotto were with the Department of Industrial Engineering, Università degli Studi di Padova, Italy (e-mail: name.surname@unipd.it).

M. Nicora[1], D. Mestriner[1], M. Brignone[2], and R. Procopio[2] were with ICT and Electrical Engineering Department, University of Genoa I-16145, Genoa, Italy (e-mail: [1]name.surname@edu.unige.it, [2]name.surname@unige.it).

M. Rubinstein was with the Institute for Information and Communication Technologies, Haute Ecole d'ingénierie et de Gestion du Canton de Vaud, 1401 Yverdon-les-Bains, Switzerland (e-mail: marcos.rubinstein@heig-vd.ch)

IV aims at presenting and discussing the obtained results (current distributions and radiated EM fields). Finally, some conclusions are drawn in Section V.

II. Lightning Return Strokes to Tall Structures

The interaction of lightning with tall strike-objects has received considerable interest in the last two decades (e.g., [20]) and several return-stroke models have been proposed (see [21] for a review). The models are extensions of those originally developed for the case of return strokes initiated at ground. The presence of a tall strike-object has been considered in two classes of return stroke models, the engineering models and the electromagnetic or Antenna-Theory (AT) models, as defined in [22].

Engineering models generally assume two current pulses injected in both directions (the strike object and the lightning channel). The upward wave propagates along the channel at the imposed return-stroke speed (usually between one third and half of the light speed). The downward wave propagates at the speed of light along the strike object, represented as a lossless uniform Transmission Line (TL) characterized by constant reflection coefficients at its extremities, which are estimated a priori from experimental results and/or general considerations. More general and straightforward formulations of these models have been allowed by either a distributed-source representation of the channel [23], or a lumped series voltage source at the junction point between the channel and the strike object [24]. Expressions for calculating the reflection coefficients as a function of frequency at the bottom of the strike object were presented in [25]. TL approaches have been successfully applied to tall structures with complex geometries, such as transmission towers (pylons) [26]–[28].

In AT models (e.g., [29], [30]), instead, the strike object is represented by a wire structure and the lightning channel by a lossy vertical wire antenna. The lightning current is injected by a voltage source at the interface channel-strike object and the Maxwell's equations are solved using a numerical method such as the Method of Moments (MoM) [31]. To reproduce a current wave speed of propagation in the channel consistent with available optical observations (i.e., values lower than the speed of light in vacuum), different channel representations have been proposed in the literature with the use of techniques aimed at artificially reducing the propagation speed [32]. A perfectly conducting ground is typically assumed, even though the ground finite conductivity and the earthing system of the tall structure were considered in some analyses (e.g., [33], [34]).

A number of transient analyses of WT under lightning strikes have been proposed in the literature. Most studies are based on the TL modelling approach and the EMTP-ATP (Electromagnetic Transients Program - Alternative Transient Program) software is used to simulate a lightning strike to one of the WT blades [19], [35]–[37]. The adoption of the TL approach requires the determination of reflection coefficients at the extremities of the strike object and at its main internal structural discontinuities, which could be challenging for complex tall structures such as WTs. This may affect the accurate evaluation of the lightning current along the WT components, leading to misunderstanding of the phenomenon.

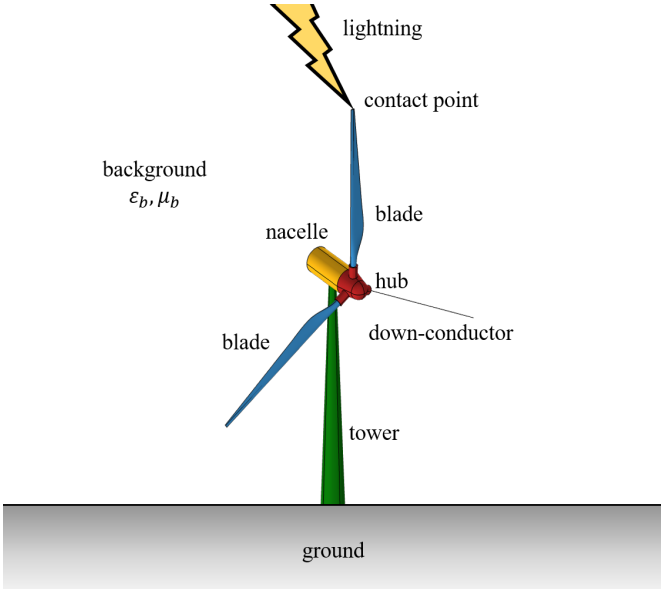

Fig. 1: Model of the lightning-return stroke to the WT (one blade has been hidden in order to show the internal down-conductor).

Therefore, in this paper, a full-wave model of the WT transient response to direct lightning strikes is proposed and thoroughly described in Section III. Actually, the full-wave approach allows considering a complete and accurate model of the WT, with real geometries and materials, without imposing restrictive approximations. Especially when experimental measurements are not available, the full-wave modelling approach may be more appropriate than the empirical formulae used for the calculation of the characteristic impedance of WT components that are used in some TL theory-based studies (e.g., [37], [38]).

III. Modeling Wind Turbines Struck by Lightning

In this section, the numerical model and the methods adopted for the transient analysis of lightning-return strokes to the WT are presented.

A. Model Description

Fig. 1 shows an exemplification of the model, i.e., a lightning-return stroke to a horizontal-axis new generation WT. The struck blade is aligned with the tower and oriented upward. In the following, the case with the struck blade inclined by 60° with respect to the tower axis is considered too. The WT model consists of the following parts: three 67 m long blades made of Glass Fiber Reinforced Polymer (GFRP), a 6 m diameter hub made of cast iron, a 20 m long nacelle made of GFRP shells, and a 99 m tall tower made of structural steel. A copper down-conductor is installed inside the blade and connected with the hub in order to provide a conductive path for the lightning current. The down conductor diameter is set to the minimum value recommended in [16] (8 mm). Table I lists the WT component geometry (diameter

TABLE I: WT model data: geometry and materials.

WT component	thickness [mm]	material	σ [S/m]
blades	50	GFRP	10^{-2}
hub	100	cast iron	$2{\cdot}10^{6}$
nacelle	30	GFRP	10^{-2}
tower	30	structural steel	$4\cdot10^{6}$
down-conductor	8 (diameter)	copper	$6\cdot10^{7}$

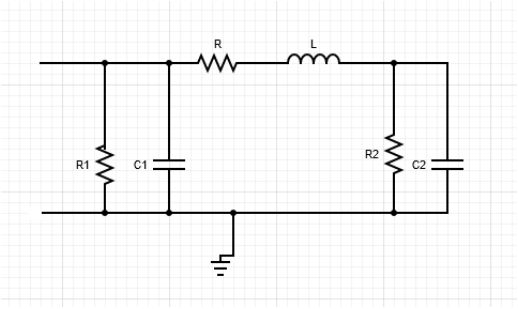

Fig. 2: Grounding system equivalent circuit

for the down-conductor, thickness for the other parts) and the conductivity values, σ, of each component.

The other main parts of the model are the lightning channel and the ground. The lightning channel is modelled as a long vertical straight cylinder of 0.1 m radius with an electrical resistance per unit length of 0.07 Ω/m, in accordance with [39]. Even if, in principle, the channel radius and per unit length resistance could be somehow affected by the peak current in a non-linear way, lightning return stroke models are known to predict with good accuracy the electromagnetic fields from lightning without adding the complexity of the mentioned non-linearities. Moreover, since the aim of this work is to evaluate if WT enhances the effects of lightning strikes, we decided to assume a model for the lightning channel which has been deeply validated in previous work.

The grounding system of the WT is adapted from the circuit described in [40] considering a CP20 grounding configuration installed in a soil characterized by a ground conductivity of 1 mS/m and a relative permittivity of 10. The equivalent grounding system is a π-circuit, described in Fig. 2. The parallel and series resistances R_1, R_2 and R are respectively, 28.75, 137.35 and 9.54 Ω. C_1 and C_2 are 1.07 and 5.66 nF, while the series inductance L is 12.5 μH. Then, the assumption of Perfect Electric Conductor (PEC) ground is adopted for the calculation of the electromagnetic fields in accordance to many works in the literature (e.g., [29], [30]). The lightning channel and the WT are connected at the contact point as shown in Fig. 1, which is chosen as the vertex of the vertical blade, where also the down-conductor is connected to the blade. In addition to the WT and the lightning channel, the other parts of the model are the ground and the background medium (i.e., the air). The modeling of each of these parts requires a particular attention and is thoroughly discussed in Section III-D. Moreover, the ensemble of WT and lightning channel is electrically long, therefore a suitable numerical method must be chosen in order to consider the time delay propagation of the EM fields.

Please note that in this framework, the upward connecting leader from the WT to the downward connecting leader has not been modelled since we are mainly interested in the evaluation of the EM fields during the return stroke phase, which is commonly regarded as the most critical one. In order to verify the negligibility of the effect of long upward connecting leaders, we performed simulations assuming an upward connecting leader of length 100 m using the bidirectional return stroke model of Willett et al [41]. The results (not presented in this paper) show that the effect is indeed negligible.

B. Numerical Method

Due to the open boundary nature of the problem and the need of studying fast transient phenomena for electrically long structures, the target problem is particularly tricky from a computational point of view.

For these reasons, the well-known Finite Element Method (FEM) is not the best solution since it would require the modelling of a very large domain which includes the WT and the lightning channel that, as will be discussed in the following, must be several kilometers wide. Moreover, the FEM would require sophisticated boundary conditions in order to avoid spurious reflections of the electromagnetic fields.

Thus, in this paper, we decided to use and implement an ad-hoc Integral Equation Method (IEM) which, contrary to FEM, only requires the meshing of the active regions, i.e., the WT and the lightning channel (therefore avoiding the discretization of the background, i.e., the air). Moreover, Integral Equation Methods naturally impose the correct boundary condition at infinite distance.

Several IEMs exist, such as the well known Method of Moments (MoM) or the Hybrid Electromagnetic Model (HEM) [42]. However, for its generality and for the simplicity of including lumped circuit elements in the full-Maxwell EM problem, the Partial Element Equivalent Circuit (PEEC) scheme has been chosen for the implementation of the method [43], [44]. In this paper, transient analyses are carried out, and therefore a time-domain version of the PEEC method based on the Marching On-In-Time (MOT) scheme is adopted [45], [46].

The choice of using a time-domain method with respect to a frequency-domain approach is justified by the following reasons: *i*) when a transient analysis is addressed by applying the Fast Fourier Transform (FFT) and the Inverse-FFT (IFFT), one should consider that the time-window chosen for the IFFT must be long enough to allow all transients to be extinguished. However, in general, it is not easy to know a priori how long such time window should be, and therefore a computationally expensive trial and error process is required. Moreover, *ii*) when the transient analysis is carried out by means of FFT and IFFT, the spurious reflections due to the finite length of the channel must be considered in the chosen time-window. Therefore, in order to avoid fictitious results, the lightning channel should be taken long enough to allow for currents which reflect when they reach the top of the channel to be

extinguished during the chosen time-window (please note that considering a 50 μs time window and a return stroke propagation speed $v_{lc} = \frac{c_0}{2}$ the channel length is 7.5 km). Alternatively, one should impose a proper termination of the lightning channel, which is no-doubt a difficult task. Finally, *iii*) it is useful to remark that, contrarily to other works, where the strike object is represented with an oversimplified model, an accurate model of the WT is used in this paper. This significantly increases the computational complexity of the simulations when the FFT and IFFT are adopted.

C. Time Domain Approach

The MOT-PEEC method starts from the well-known Electric Field Integral Equation (EFIE) [43], i.e.,

$$\mathbf{E}(\mathbf{r},t) = -\frac{\partial \mathbf{A}(\mathbf{r},t)}{\partial t} - \nabla\varphi(\mathbf{r},t) + \mathbf{E}_{inc}(\mathbf{r},t), \quad (1)$$

where $\mathbf{E}$ is the electric field, $\mathbf{A}$ is the magnetic vector potential, φ is the scalar electric potential, $\mathbf{E}_{inc}$ is the known incident electric field and $\mathbf{r}$ is the field point. In the EFIE equation, $\mathbf{A}$ and φ are given by integral expressions in terms of the current density vector ($\mathbf{J}$) and the charge density (ϱ) [45]. In the PEEC scheme, (1) is complemented by the Ohm's law

$$\mathbf{E}(\mathbf{r},t) = \mathbf{J}(\mathbf{r},t)/\sigma(\mathbf{r}), \quad (2)$$

where σ is the electric conductivity. Moreover, the continuity equation is also imposed

$$\nabla \cdot \mathbf{J}(\mathbf{r},t) = -\frac{\partial \varrho(\mathbf{r},t)}{\partial t}. \quad (3)$$

Then, the current density vector $\mathbf{J}$ and the scalar electric potential φ are chosen as problem unknowns and they are expanded by means of space shape functions and temporal shape functions as in [45]. In particular, facet shape functions (i.e., RWG shape functions) are used for the space discretization of $\mathbf{J}$, whereas φ is expanded with piecewise constant shape functions. Simple hat (i.e., triangular) shape functions are used for the temporal discretization by following a leap-frog scheme for $\mathbf{J}$ and φ. A Galerkin approach is then applied to (1)–(3) for the space discretization and a collocation method is applied for the temporal discretization. This leads to the following MOT-PEEC scheme

$$(\mathbf{R}+\mathbf{L}_0)\mathbf{j}^{(s)} + \frac{1}{2}\mathbf{A}^T\phi^{(l)} = \mathbf{e}_{inc}^{(s)} - \sum_{u=1}^{H_T}(\mathbf{L}_u\mathbf{j}^{(s-u)}) - \frac{1}{2}\mathbf{A}^T\phi^{(l-1)}, \quad (4)$$

$$\mathbf{P}\mathbf{A}\mathbf{j}^{(s)} - \frac{1}{\Delta_T}\phi^{(l)} = -\sum_{u=1}^{H_T}(\mathbf{P}_u\mathbf{A}\mathbf{j}^{(s-u)}) - \frac{1}{\Delta_T}\phi^{(l-1)}. \quad (5)$$

where $\mathbf{R}$, $\mathbf{L}_k$, and $\mathbf{P}_k$, with $k = 0, \cdots, H_T$ are the resistance, inductance, and potential MOT-PEEC matrices, respectively, whereas $\mathbf{A}$ is the incidence matrix of the equivalent circuit [43] (i.e., $\mathbf{A}$ and $\mathbf{A}^T$ are the discrete equivalent of the divergence and gradient operators, respectively). $\mathbf{j}$, ϕ and $\mathbf{e}_{inc}$ are the arrays corresponding to $\mathbf{J}$, φ, and $\mathbf{E}_{inc}$, respectively. In the equations above, Δ_T is the chosen time step for the temporal discretization, superscripts indicating the time instant (e.g., $\mathbf{j}^{(s)}$ is the current array at time instant $t_s = s\Delta_T$ and $\phi^{(l)}$ is the electric potential array at time instant $t_l = l\Delta_T$, where $t_l = t_s + \Delta_T/2$), and matrices $\mathbf{L}_u$ and $\mathbf{P}_u$, with $u = 1, \cdots, H_T$, represent the electromagnetic interactions between unknowns at the time instant s and at the previous time instant $s-u$. When $u = 0$, these matrices represent instantaneous interactions between unknowns at the same time instant. On the other hand, when $u > 0$, these matrices represent retarded interactions between unknowns that are separated in time by a quantity equal to $u\Delta_T$. $H_T = \lceil 1 + D_{max}/(\Delta_T v) \rceil$ indicates how many previous time steps actually interact with the present solution, where D_{max} is the maximum distance between two mesh elements and $\lceil \cdot \rceil$ is the ceiling operator. More details concerning the MOT-PEEC method can be found in [45], where a graphical representation of matrices is also given. The left-hand side of (4) and (5) consists of resistance, incidence, and sparse instantaneous matrices only (i.e., the ones with $u = 0$) and it is the same for each time step. The right–hand side is instead updated at each time step by multiplying the sparse marching matrices (i.e., the ones with $u = 1, \cdots, H_T$) with the previous H_T solutions.

Inductance and potential matrices store the instantaneous and retarded electromagnetic interactions between all the unknowns of the discrete problem. Their coefficients (which are fully reported, e.g., in [45]) depend on the Green's function of the background, i.e.,

$$L_{u,kh} = \mu_b \int_\Omega \int_\Omega \frac{\mathbf{w}_k(\mathbf{r}) \cdot \mathbf{w}_h(\mathbf{r}') \frac{\partial T(t_u)}{\partial t'}}{4\pi||\mathbf{r}-\mathbf{r}'||} d\Omega' d\Omega, \quad (6)$$

where $\mathbf{w}$ is the space shape function, T is the temporal shape function, $\mathbf{r}'$ is the source point and and $t' = t - \frac{||\mathbf{r}-\mathbf{r}'||}{v}$ is the retarded time, with $v = \frac{1}{\sqrt{\varepsilon_b \mu_b}}$ being the speed of light in the background medium (with ε_b and μ_b being the permittivity and permeability of the background medium). In (6), t_u is the discretized retarded time $t_u = u\Delta_T - \frac{||\mathbf{r}-\mathbf{r}'||}{v}$.

D. Modeling Issues and Challenges

Due to the electrical length of the model, which consists of different parts that require specific attention, several modeling issues must be addressed. These issues are thoroughly discussed in the following.

1) Reduced Propagation Speed in the Lightning Channel: As previously mentioned, the propagation speed of the current in the lightning channel is lower that the speed of light in vacuum and its value is largely independent of the lightning current [47]. However, the reasons for this reduced propagation speed are not completely known and they are probably due to non-linear local phenomena that occur in the lightning channel. Since they are unknown and local, this kind of phenomena cannot be exactly modelled. Moreover, a detailed modelling of the propagation speed varying with geometrical and electrical parameters (such as the lightning

current) is out of the scope of this work, which aims at evaluating the possible enhance of the lightning effects due to the presence of the WT. However, it is important to correctly impose the reduced propagation speed. To achieve this, we have adopted the idea of [39], where the background is replaced by an artificial dielectric medium with a relative permittivity $\varepsilon_r = 5.3$ so that

$$v_{lc} = \frac{1}{\sqrt{\varepsilon_r \varepsilon_0 \mu_0}} = 1.3 \cdot 10^8 \text{ m/s}, \tag{7}$$

where ε_0 and μ_0 are the permittivity and permeability of vacuum, respectively.

However, in [39], only the lightning channel was considered. In this work, the WT is also considered where the propagation speed of currents is the one of vacuum, i.e., c_0.

Thanks to the use of an Integral Equation Method, it is possible to adopt different propagation speeds in different parts of the model. Indeed, the coefficients of the inductance and potential matrices depend on the properties of the background region (i.e., permittivity and permeability). Therefore, to allow different propagation speeds, we impose a background with the properties of vacuum for the self and mutual coefficients of the unknowns belonging to the WT, whereas we impose a background with $\varepsilon_r = 5.3$ for the self and mutual coefficients belonging to the lightning channel. Mutual coefficients between the WT and the lightning channel are computed considering a background with the properties of vacuum. Indeed, while currents in the channel propagate at a reduced speed due to local phenomena, the radiated electromagnetic fields that account for the mutual couplings propagate in vacuum at c_0. In short, the idea is that the WT sees a background with $\varepsilon_b = \varepsilon_0$ and $\mu_b = \mu_0$, whereas the lightning channel sees a background with $\varepsilon_b = \varepsilon_r \varepsilon_0$ and $\mu_b = \mu_0$, with $\varepsilon_r = 5.3$.

It is worth noting that, once the MOT-PEEC simulations are performed, the distribution of $\mathbf{J}$ is known and the radiated electromagnetic fields can be evaluated in post processing by means of classical integral expressions [17], [30], [39]. At this point, the electromagnetic fields generated by currents flowing both in the WT and in the lightning channel are evaluated considering the real background (i.e., $\varepsilon_b = \varepsilon_0$ and $\mu_b = \mu_0$). Indeed, the radiated electromagnetic fields propagate in vacuum at c_0, even if the source currents in the channel travel with a reduced propagation speed.

2) Excitation: Lightning return strokes to tall objects are mainly studied by means of engineering models [21] in which the channel current is expressed analytically, such as the Modified Transmission Line (MTL) approach [48], [49]. Typically, a current source is injected at the interface between the channel and the tall structure (e.g., [17], [25]). The assumed current source is the channel-base current for ground-initiated return strokes, usually reproduced by means of the Heidler's function [50]. The injected pulse propagates upward in the channel at the imposed return-stroke speed (between one third and half of the speed of light) and downward in the object at the speed of light. The object is modeled as an ideal transmission line characterized by reflection coefficients at its extremities. Other engineering models (e.g., [24]) adopt a voltage source with the voltage magnitude being expressed in terms of the lightning short-circuit current and equivalent impedance of the lightning channel. In any case, for engineering models, the time evolution of the current at the injection point is given by the injected one plus the terms due to transmissions and reflections. Of course, the results are reasonable only if the reflection coefficients (which are inputs to the engineering models) are known with a good confidence.

On the other hand, when a full-Maxwell approach is applied, if we directly impose the Heidler's waveform for the return-stroke current at the injection, we are also distorting/enforcing the reflection and the transmission of currents at the interface between the WT and the channel, thus actually forcing the *total* current (i.e., the one resulting from the combination of injection and reflections/transmissions) to be the Heidler's current. Instead, several experimental results (see e.g., [30, Fig. 2]) have shown that the total current at the top of the structure (or in close proximity) is affected by multiple reflections and transmissions which occur along the tall object and at ground level.

Therefore, when performing a full-Maxwell simulation, it is clear that we need to impose a voltage excitation which, unfortunately, is not known a priori.

In order to solve this tedious problem, the approach described in the following was adopted and results were compared against experimental data and simulation results from other methods in the literature where other tall objects struck by lightning are considered (e.g., the well-known CN tower case in Toronto [17], [30]).

The main idea is to model the lightning-return stroke as a voltage-driven phenomenon (as in [30]) where the applied voltage is derived from a previous simulation where the return stroke initiates at ground level (i.e., without the presence of the tall of object). However, numerical simulations have shown that if one directly applies the voltage obtained from this simulation to the tall-object case, an undesired attenuation of the injected current is obtained. This should be expected since the equivalent impedances seen from the excitation point are obviously different in the two cases (i.e., ground-only case and tall-object case). Therefore, in order to impose the desired current, the voltage obtained from the ground-only case is scaled so that the injected current reaches the desired peak value. This approach is similar to the one in [30]. However, in this paper the approach is performed directly in time-domain instead of working in frequency domain. By doing so we are, at the same time, injecting the current with the desired peak value and allowing natural reflections between the WT and the channel. Therefore, in the same fashion of the MTL approach, the time evolution of the current at the injection point is given by the injected one plus the terms due to transmissions and reflections. The approach is exemplified in Fig. 3 and can be summarized in the following steps:

1) the case of a return stroke which initiates at ground level (i.e., without the WT) is simulated by imposing the desired channel-base current;

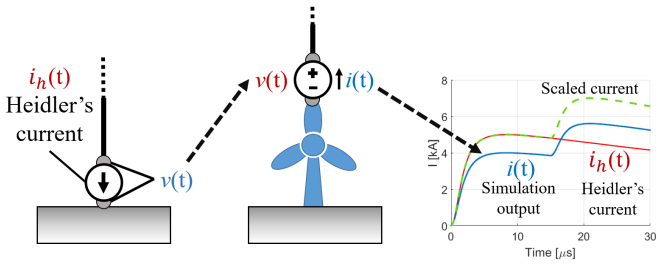

Fig. 3: Simulation flowchart. Red: imposed quantity. Blue: computed quantity.

2) from the results of this simulation, the time-domain voltage between the ground point (where the stroke initiates) and the channel base is evaluated;
3) this voltage is then applied as the excitation of the simulation where the WT is considered;
4) finally, results are scaled in order that the current before the occurrence of the first reflection is the desired one according to [51]. Please note that, if an electrically short tower is considered, it is necessary to reduce the time-step size in order to correctly catch the occurrence of the first reflection.

With the proposed approach, we remark that, contrary to TL approaches where reflections coefficients are imposed a priori, reflections and transmissions are naturally considered (with a reasonable numerical accuracy), and this is one of the main advantages of using a full-Maxwell technique. The results in terms of current distribution and radiated electromagnetic fields obtained from this procedure are in very good agreement with experimental data and simulation results when applied to the well-known CN tower case [30].

3) Skin Effects: The last issue which must be considered is the skin depth in the metallic structures of the WT. In this problem, transients are so fast that the skin effect is very pronounced, i.e., the currents are mostly concentrated on the skin of the conductive devices. However, the skin depth varies during the transient and it is not clear a priori if this variation should be considered or not. To study that, in this paper we have carried out numerical experiments using the approach proposed in [52], which allows for considering the variation of the skin depth during the transient. Fortunately, numerical experiments have shown that results in terms of current distribution and radiated EM fields were substantially the same by using [52] or by applying the PEC assumption for all the components of the WT. Indeed, during fast transients, the self impedance of the PEEC elements is dominated by the inductive term, whereas the resistive term (which strongly depends on the skin depth) has a negligible impact. Therefore, the PEC assumption has been used.

IV. Results and Discussion

This section focuses on discussing the current distribution along the channel and along the WT and, secondly, the EM fields at two representative distances (500 m and 2000 m) from the WT. In the following, both the first and subsequent stroke cases will be analyzed. The system is excited by a voltage source, whose time-domain waveforms (for first and subsequent strokes) are presented in Fig. 4. Please note that the definition of the proposed voltage sources has been obtained following the procedure presented in Section III, adopting the classical parameters for the Heidler's function in case of first and subsequent strokes [50]. Specifically, the parameters reported in Table II [17] have been used in this paper. The results obtained with the presence of the WT are also compared with the case of a lightning directly striking the ground, where the Heidler's current at the base of the channel is directly imposed.

Concerning the computational cost, the construction of each marching inductance/potential matrix required about 20/30 s whereas each time step solution required about 2 s. 18014 mesh elements were used to discretise the model and the chosen time step was 30 ns. The number of marching matrices, i.e. H_T, was 3402 and the number of simulated time steps was 2000. Once the time-domain current distribution was obtained, the EM fields were evaluated in post-processing with a computational cost which was negligible with respect to the one required for the solution of the MOT-PEEC problem (about 5 minutes). The simulations required about 8 GB of RAM and were performed in a Linux machine equipped with a Xeon E5-2643 v4 processor (dual 6-core/12-thread, @3.40 GHz) and 512 GB of RAM.

In the following figures, the observation point of the current along the WT refers to the height above the ground (which varies from 0 m to 170 m), but the current path is slightly longer since the wave runs also along the nacelle of the WT, which is placed horizontally.

Please note that the analysis has been performed taking into account two different positions of the struck blade: *i*), the struck blade is aligned with the tower axis and oriented upward and *ii*) the struck blade is inclined by 60° with respect to the tower axis.

Simulation results have shown that, in terms of current distributions along the channel and along the WT, the inclination of the struck blade has a negligible effect. For this reason, in Section IV-A, the results are presented only for the case referring to the vertical struck blade.

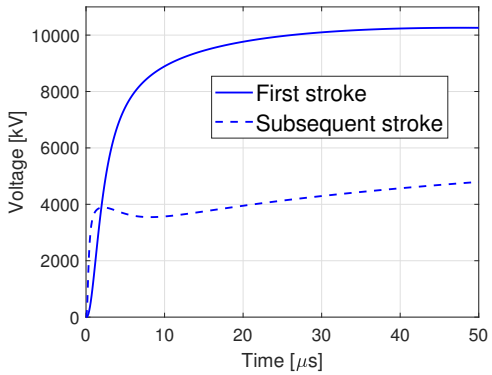

Fig. 4: Voltage source placed at the WT-lightning channel.

TABLE II: Heidler's function parameters [17].

Return stroke	I_{01} [kA]	τ_{11} [μs]	τ_{21} [μs]	N_1	I_{02} [kA]	τ_{12} [μs]	τ_{22} [μs]	N_2
First	28.0	1.80	95	2	-	-	-	-
Subsequent	10.7	0.25	25	2	6.5	2	230	2

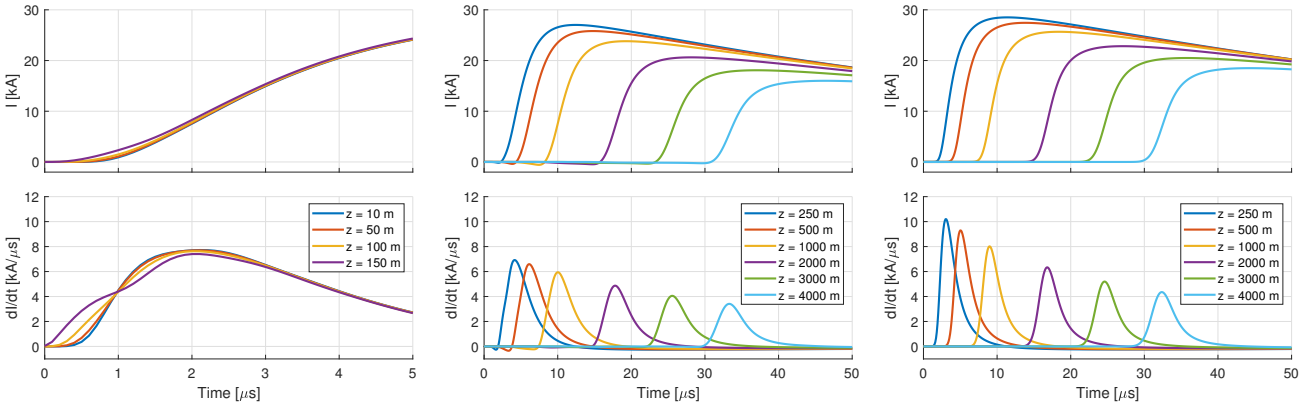

(a) WT (b) Channel (c) Channel - No WT

Fig. 5: Current and current derivative along the WT and along the channel - First return stroke.

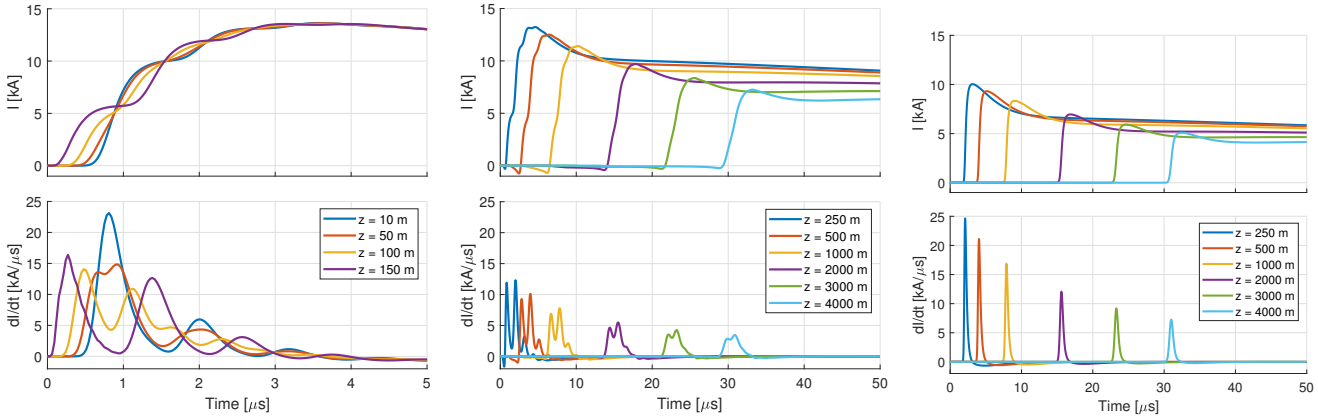

(a) WT (b) Channel (c) Channel - No WT

Fig. 6: Current and current derivative along the WT and along the channel - Subsequent return stroke.

On the other hand, concerning the radiated EM fields, the inclined blade position plays an important role when the subsequent stroke is considered, as shown later in Section IV-B.

A. Current Waveform

The first return return stroke case is analyzed in Fig. 5. The current along the WT and its time derivative are shown in Fig. 5a for the first 5 μs (after this value no meaningful differences between the currents can be observed) and show one main reflection due to the ground, while the discontinuities due to the other parts of the WT and due to the connection between the WT and the channel seem to have negligible effect on the current waveform. Referring to the well-known TL-based approach [17], for the range of frequencies representative of the first stroke, the presence of the WT has a negligible effect and it can be disregarded or represented by a lumped impedance (electrically small).

It is interesting to notice that the current along the WT is slightly distorted while it propagates (as shown in the bottom plot of Fig. 5a, the waveform becomes faster while it approaches the ground), while the peak attenuation cannot be evaluated correctly since the first reflection arrives earlier than the time-to-peak.

Even if not presented for the sake of brevity, it should be noted that the maximum peak reached by the current in each point of the tower (excluding the blade) is lower than

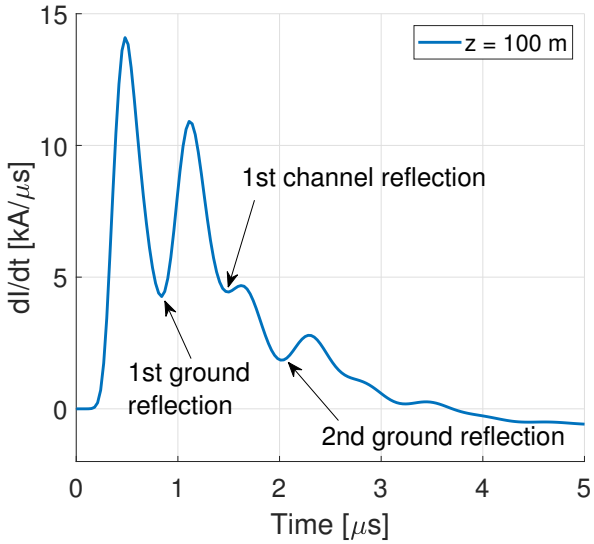

Fig. 7: Current derivative at $z = 100$ m along the WT - Subsequent return stroke.

30 kA. The attenuation of the current is mainly caused by the reflection occurring at the ground discontinuity. Since the grounding is modelled with an equivalent circuit, the reflection coefficient is not unitary as in the PEC ground case, thus only a part of the current is reflected upwards. The attenuation along the tower is negligible during both the upward and downward propagation processes; that could be ascribed to the relatively short length of the WT.

The current along the channel (top panel of Fig. 5b) is characterized by an attenuation and a distortion of the waveform while it propagates along the channel. These results are in accordance with [39], where only the channel was analyzed. On the other hand, in this case the distortion of the lightning current seems to be less evident as the maximum derivative shows a slower decrease at higher altitudes with respect to the case without the WT. This is confirmed by the comparison between the bottom panel of Fig. 5b and Fig. 5c: considering the WT leads to a 50% decrease of the maximum derivative from 250 m and 4000 m, while the decrease in the case of lightning striking the ground reaches 58%.

On the other hand, the attenuation along the channel is more evident when the WT is considered. This can be clearly noticed from the top panel of Fig. 5b and Fig. 5c. While a 35% peak current decrease is observed from 250 m to 4000 m if the WT is not considered, such value reaches 40% when it is included in the simulation. The different behaviour in terms of distortion and attenuation along the lightning channel could be ascribed to the mutual EM coupling effects between the WT and the channel. Moreover, the current along the channel is affected by a phenomenon occurring in the early stages of the current propagation: as shown in Fig. 5b, in the first few μs the sign of the current becomes negative. This aspect is mainly related to the mutual coupling between the WT and the channel. The current propagates along the WT at the speed of light and its radiation field induces a negative current on the channel. This negative current is mainly visible until the wave-front (propagating at v_{lc} along the lightning channel) arrives at the observation point.

The analysis of the subsequent stroke is presented in Fig. 6 and leads to conclusions similar to those for the first stroke case. However, in this case, the reflections occurring along the WT are not only related to the ground discontinuity.

Let us consider the current derivative at 100 m (Fig. 7): the first reflection occurs at 0.9 μs, which corresponds to the ground reflection; a second reflection can be observed at 1.37 μs and can be ascribed to the current reflected at the discontinuity between the WT and the channel; later on, other reflections are observed and are related to the subsequent reflections from ground and WT top. This leads to the conclusion that, for the range of frequency characterizing the subsequent stroke, the discontinuity between the WT and the channel should be considered in a TL modelling approach.

The current along the WT presents a slight and similar attenuation in both propagation directions; such behaviour is the expected one for cylindrical structures or conical structures with small base radius [53]. The distortion along the WT can be evaluated from the bottom panel of Fig. 6a, where the peak of the current derivative decreases during the time window before the occurrence of the first ground reflection.

The current along the channel is clearly distorted and attenuated during the propagation. Comparing the results with the ones obtained without the WT (Fig. 6c) it can be noticed that the current peak and the current derivative peak have similar percentage decrease in both cases.

B. Electromagnetic Fields

The current distributions in the WT and in the lightning channel are used in this subsection to calculate the radiated EM fields by using classical integral expressions [17], [30].

The electric field is made of three terms. These terms involve the time integral of the current density, the current density itself (or, equivalently, the time derivative of the charge density), and the time-derivative of the current density and they are named electrostatic, induction, and radiation terms, respectively. The magnetic field has the induction term and radiation term only.

Computed electric fields at ground level, at two different distances (500 m and 2000 m), for the first and the subsequent return stroke cases are shown in Fig. 8. The vertical position of the struck blade is considered. In each panel, the WT blade-tip initiated return stroke E-field (solid line) is depicted together with the corresponding ground initiated return stroke E-field (dashed line). Fig. 9 is the analogous for the computed magnetic fields. In these figures, the induction, radiation and electrostatic (if present) components are shown separately.

It is well known that the contribution of the different components of the electric and magnetic fields is strongly affected by the observation point distance. The radiation term contribution to the total field increases with the distance. At closer observation points (a few hundred meters) static and induction effects are predominant. On the other hand, at large distances, (beyond some tens of kilometers) the static

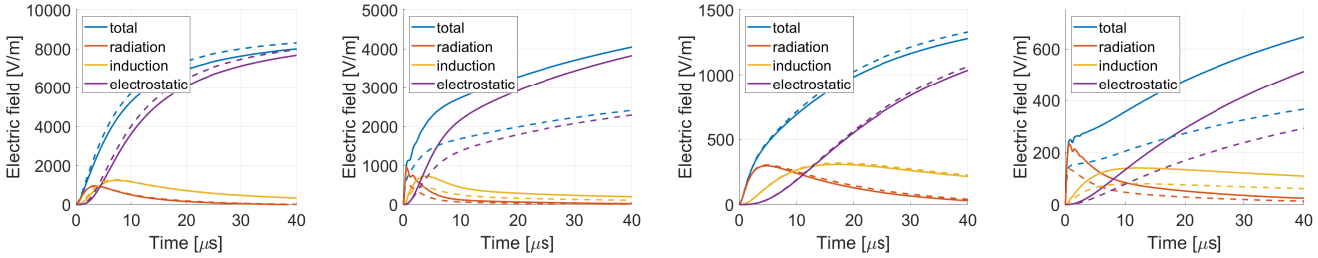

(a) First stroke - $r = 500$ m (b) Subsequent stroke - $r = 500$ m (c) First stroke - $r = 2000$ m (d) Subsequent stroke - $r = 2000$ m

Fig. 8: Vertical electric field at ground level, at two distances r, for first and subsequent return strokes to the WT (solid line) and to the ground (dashed line).

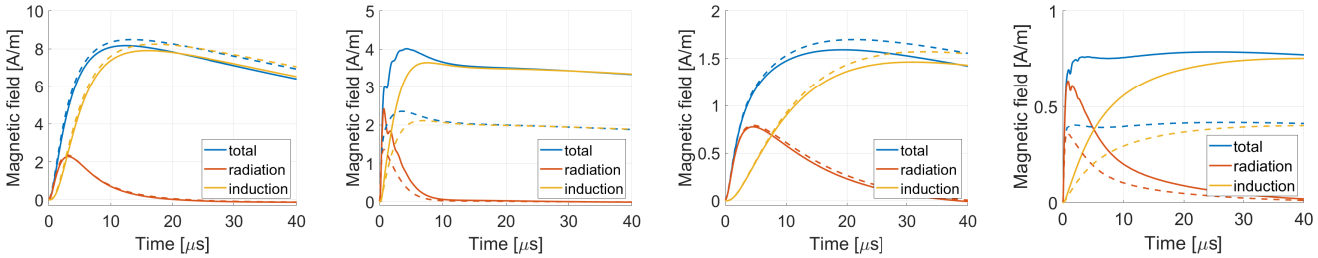

(a) First stroke - $r = 500$ m (b) Subsequent stroke - $r = 500$ m (c) First stroke - $r = 2000$ m (d) Subsequent stroke - $r = 2000$ m

Fig. 9: Azimuthal magnetic field at ground level, at two distances r, for first and subsequent return strokes to the WT (solid line) and to the ground (dashed line).

and induction effects are negligible [54]. The obtained EM fields are consistent with such features. The radiation-term contribution to the total field is more significant at 2000 m (Fig. 8cd and Fig. 9cd) than at 500 m (Fig. 8ab and Fig. 9ab).

Concerning return strokes initiated at ground level, one can observe that the first stroke electric field waveform (dashed lines in Fig. 8ac) consists in an initial fast-rising ramp, essentially due to the radiation term, and then a less steep increase associated to the static term. The subsequent stroke E-field (dashed lines in Fig. 8bd) is characterized by an initial peak caused by the behaviour of the radiation term. Both first and subsequent stroke magnetic fields (dashed lines in Fig. 9) show an initial ramp, due to the radiation term, followed by a gradual decay, mainly induction-driven. However, for the subsequent-stroke case, the peak is more pronounced and reached earlier. The subsequent return stroke current waveform has lower time-to-peak and higher maximum steepness compared to the first return stroke. Therefore, the contribution of the radiation term to the total E-field and H-field is more significant for the subsequent stroke case.

For return strokes initiated at the WT blade tip, by observing the E-fields (solid lines in Fig. 8) and the H-fields (solid lines in Fig. 9), it is possible to state that the presence of the WT does not result in any amplification effect for the first stroke: a slight decrease is observed due to the presence of the grounding system. Whereas, both at 500 m and 2000 m, the magnitude of the EM fields associated with the subsequent stroke initiated at the blade tip of the considered WT is increased by a factor 1.7-1.8 with respect to the corresponding subsequent return stroke initiated at ground level.

The presence of the WT causes the occurrence of field waveform oscillations due to current reflections along the WT. Such reflections can be identified especially on the radiation term of the subsequent stroke electromagnetic fields (solid line in Fig.8bd for the E-field and in Fig. 9bd for the H-field).

The maximum steepness of the EM waveforms is reported in Table III for the E-field and the H-field, for all the considered combinations. One can observe that the WT causes increased values for the maximum steepness of the subsequent return stroke EM fields; the increase factor is 1.7-1.8. On the other hand, no variations appear for the first return stroke.

The effect of the relation between the structure height and the current time-to-peak on the EM fields is investigated for the subsequent return stroke case by repeating the simulation with a scaled-up WT (total height 268 m) and the same current waveform parameters (Table II) adopted to find the excitation voltage waveform. No significant variations are observed in the EM fields waveforms. This result is consistent with those reported in [55]: when the current time-to-peak is lower than $2h/c_0$ (h being the elevated strike object height), the field enhancement factor can be expressed in terms of the return stroke speed, the speed of light in vacuum, and the current reflection coefficient at the top of the elevated strike object. Hence, h is not directly involved.

Finally, the effect of the struck blade rotation angle on the EM fields is investigated. Only the subsequent return stroke case is considered, since it was found that the presence of the WT produces negligible effects for the first return stroke

TABLE III: EM fields maximum steepness.

Waveform	Unit	First return stroke		Subsequent return stroke	
		WT initiated	Ground initiated	WT initiated	Ground initiated
E-field at 500 m	V/m/μs	753.5	860.7	3205.9	1851.9
E-field at 2000 m	V/m/μs	155.8	159.1	814.0	445.2
H-field at 500 m	A/m/μs	1.9	2.0	8.7	4.9
H-field at 2000 m	A/m/μs	0.4	0.4	2.2	1.2

TABLE IV: Parameters of subsequent return stroke EM fields at 10 m above the ground with two different struck blade angles.

Waveform	Parameter	Unit	$r = 500$ m		$r = 2000$ m	
			Blade angle 0°	Blade angle 60°	Blade angle 0°	Blade angle 60°
Vertical E-field	Maximum value	V/m	4290.0	4933.1.0	668.6	695.2
	Initial peak value	V/m	1088.5	1185.6	247.7	257.3
	Time-to-initial peak	μs	0.7	0.8	0.8	1.0
Radial E-field	Maximum value	V/m	97.0	127.8	5.7	5.7
Azimuthal H-field	Maximum value	A/m	4.0	4.5	0.8	0.8

case.

Table IV reports the EM fields waveform parameters at 500 m and 2000 m distance with two different struck blade angles with respect to the tower axis (0° and 60°) at 10 m above the ground, in order to observe also the radial component of the electric field which may affect the magnitude of the induced overvoltages on overhead power lines.

It can be noted that, for all cases, the field maximum value is enhanced when considering the inclined struck blade; the increase factor is more pronounced at 500 m (1.1-1.3), whereas it is almost negligible at 2000 m. Moreover, for the vertical component of the electric field, a slight increase of both the initial peak value and the time-to-initial peak is observed for the inclined struck blade case.

V. Conclusion

A full-Maxwell approach has been applied to the case of lightning striking a Wind Turbine (WT). The lightning return stroke has been modelled as a voltage source applied between the tip of the struck WT blade and the channel, whose waveform has been identified in order to provide the used Heidler's current in the time range before the occurrence of the first reflection from the ground. The implemented Integral Equation method has also allowed having electromagnetic (EM) fields propagating at the speed of light in the WT and at the typical current propagation speed in the lightning channel.

The proposed analysis has shown that, for both first and subsequent strokes, the attenuation and the distortion of the current along the channel are not negligible and comparable to the case without WT. The current waveforms are affected by the ground reflections (first and subsequent strokes) and by the reflections between the blade top and the channel (subsequent strokes only). Such reflections cause an increase by a factor 1.7-1.8 of the subsequent return stroke current propagating in the channel in the presence of the WT with respect to the case without the WT; on the other hand, no magnitude variations have been found for the first stroke case. The current along the channel is affected by a transient negative sign in the first few microseconds, due to the induced effect of the faster current flowing into the WT. The first return stroke EM fields have been computed with and without the WT, and no significant variations have been found. This is different for subsequent return strokes, whose current waveform is characterized by lower time-to-peak and higher maximum steepness than the first return stroke one. The magnitude of the subsequent return stroke EM fields is increased with respect to the case without the WT due to the fast current transient occurring into the WT caused by reflections (increase factor 1.7-1.8); the radiation term is the dominant one as it depends on the current derivative; an initial peak enhancement can be observed; the presence of the WT causes increased values for the waveforms maximum steepness (increase factor 1.7-1.8). The same results can be obtained with a 60% taller WT. The effects of the inclined position of the struck blade have been investigated. It has been shown that it does not influence the current distributions, whereas it causes an enhancement of the EM fields magnitude for the subsequent stroke case. Future research will investigate the feasibility of applying simplified models of WT in order to reduce the computational effort while maintaining accuracy. Such kind of simplified models may allow the study of a multitude of scenarios in order to identify worst case configurations. Moreover, future research will be focused on overcoming the main limitation of the present approach, i.e., the difficulty of exactly considering a realistic ground with frequency dependent parameters. This would also allow for evaluating horizontal electric fields which may cause scattered induced voltages on overhead power lines. Moreover, ad-hoc Model Order Reduction techniques will be adopted in order to reduce the overall computational complexity [56].

Acknowledgment

The authors would like to express their gratitude to Prof. Farhad Rachidi for his valuable comments and suggestions in the preparation of this paper.

References

[1] "Wind energy barometer," *EuroObserv'ER Project*, 2020.

[2] R. Alipio, D. Conceição, A. De Conti, K. Yamamoto, R. N. Dias, and S. Visacro, "A comprehensive analysis of the effect of frequency-dependent soil electrical parameters on the lightning response of wind-turbine grounding systems," *Electric Power Systems Research*, vol. 175, p. 105927, 2019.

[3] K. Yamamoto, S. Yanagawa, K. Yamabuki, S. Sekioka, and S. Yokoyama, "Analytical surveys of transient and frequency-dependent grounding characteristics of a wind turbine generator system on the basis of field tests," *IEEE Transactions on Power Delivery*, vol. 25, no. 4, pp. 3035–3043, 2010.

[4] F. Rachidi, M. Rubinstein, and A. Smorgonskiy, *Lightning Protection of Large Wind-Turbine Blades*. Springer, 01 2012, pp. 227–241.

[5] A. Smorgonskiy, F. Rachidi, M. Rubinstein, G. Diendorfer, and W. Schulz, "On the proportion of upward flashes to lightning research towers," *Atmospheric Research*, vol. 129-130, pp. 110–116, 2013.

[6] J. Montanyà, F. Fabró, O. van der Velde, V. March, E. R. Williams, N. Pineda, D. Romero, G. Solà, and M. Freijo, "Global distribution of winter lightning: a threat to wind turbines and aircraft," *Natural Hazards and Earth System Sciences*, vol. 16, no. 6, pp. 1465–1472, 2016.

[7] F. Rachidi, M. Rubinstein, J. Montanya, J. Bermudez, R. Rodriguez Sola, G. Sola, and N. Korovkin, "A review of current issues in lightning protection of new-generation wind-turbine blades," *IEEE Transactions on Industrial Electronics*, vol. 55, no. 6, pp. 2489–2496, 2008.

[8] Y. Wang, D. Yeqiang, Y. Liu, L. Qu, X. Wen, L. Lan, and J. Wang, "Influence of blade rotation on the lightning stroke characteristic of a wind turbine," *Wind Energy*, vol. 22, 08 2019.

[9] J. Montanyà, O. van der Velde, and E. R. Williams, "Lightning discharges produced by wind turbines," *Journal of Geophysical Research: Atmospheres*, vol. 119, no. 3, pp. 1455–1462, 2014.

[10] D. Wang, N. Takagi, T. Watanabe, H. Sakurano, and M. Hashimoto, "Observed characteristics of upward leaders that are initiated from a windmill and its lightning protection tower," *Geophysical Research Letters*, vol. 35, no. 2, 2008.

[11] K. Michishita, M. Furukawa, N. Honjo, and S. Yokoyama, "Measurement of lightning current at wind turbine near coast of Sea of Japan in winter," in *2016 33rd International Conference on Lightning Protection (ICLP)*, 2016, pp. 1–5.

[12] A. Candela Garolera, S. F. Madsen, M. Nissim, J. D. Myers, and J. Holboell, "Lightning damage to wind turbine blades from wind farms in the U.S." *IEEE Transactions on Power Delivery*, vol. 31, no. 3, pp. 1043–1049, 2016.

[13] K. Yamamoto, T. Noda, S. Yokoyama, and A. Ametani, "Experimental and analytical studies of lightning overvoltages in wind turbine generator systems," *Electric Power Systems Research*, vol. 79, no. 3, pp. 436–442, 2009, special Issue: Papers from the 7th International Conference on Power Systems Transients (IPST).

[14] S. Yokoyama, "Lightning protection of wind turbine blades," *Electric Power Systems Research*, vol. 94, pp. 3–9, 2013, lightning Protection of Advanced Energy Systems.

[15] K. Yamamoto, T. Noda, S. Yokoyama, and A. Ametani, "An experimental study of lightning overvoltages in wind turbine generation systems using a reduced-size model," *Electrical Engineering in Japan*, vol. 158, no. 4, pp. 22–30, 2007.

[16] "Wind turbine generator systems—part 24: Lightning protection," *IEC 61400-24*, 2019.

[17] F. Rachidi, W. Janischewskyj, A. M. Hussein, C. A. Nucci, S. Guerrieri, B. Kordi, and Jen-Shih Chang, "Current and electromagnetic field associated with lightning-return strokes to tall towers," *IEEE Transactions on Electromagnetic Compatibility*, vol. 43, no. 3, pp. 356–367, 2001.

[18] Y. Baba and V. A. Rakov, "Lightning electromagnetic environment in the presence of a tall grounded strike object," *Journal of Geophysical Research: Atmospheres*, vol. 110, no. D9, 2005.

[19] J. Birkl, E. Shulzhenko, J. Kolb, and M. Rock, "Approach for evaluation of lightning current distribution on wind turbine with numerical model," in *2016 33rd International Conference on Lightning Protection (ICLP)*, 2016, pp. 1–8.

[20] V. A. Rakov, "Transient response of a tall object to lightning," *IEEE Transactions on Electromagnetic Compatibility*, vol. 43, no. 4, pp. 654–661, 2001.

[21] F. Rachidi, "Modeling lightning return strokes to tall structures: A review," *Journal of Lightning Research*, vol. 1, 01 2007.

[22] V. A. Rakov and M. A. Uman, "Review and evaluation of lightning return stroke models including some aspects of their application," *IEEE Transactions on Electromagnetic Compatibility*, vol. 40, no. 4, pp. 403–426, 1998.

[23] F. Rachidi, V. A. Rakov, C. A. Nucci, and J. L. Bermudez, "Effect of vertically extended strike object on the distribution of current along the lightning channel," *Journal of Geophysical Research: Atmospheres*, vol. 107, no. D23, pp. ACL 16–1–ACL 16–6, 2002.

[24] Y. Baba and V. A. Rakov, "On the use of lumped sources in lightning return stroke models," *Journal of Geophysical Research: Atmospheres*, vol. 110, no. D3, 2005.

[25] J. L. Bermudez, M. Rubinstein, F. Rachidi, F. Heidler, and M. Paolone, "Determination of reflection coefficients at the top and bottom of elevated strike objects struck by lightning," *Journal of Geophysical Research: Atmospheres*, vol. 108, no. D14, 2003.

[26] L. Boufenneche, B. Nekhoul, D. Poljak, K. Kerroum, and K. El Khamlichi Drissi, "Interaction between lightning discharge and electrical tower," in *2010 30th International Conference on Lightning Protection (ICLP)*, 2010, pp. 1–6.

[27] J. A. Gutiérrez, J. L. Bermudez, F. Rachidi, M. Paolone, C. A. Nucci, W. A. Chisholm, P. Moreno, and J. L. Naredom, "A reduced-scale model to evaluate the response of nonuniform towers to a lightning strike," in *26th International Conference Lightning Protection (ICLP), Cracow, Poland*, 2002.

[28] L. Grcev and F. Rachidi, "On tower impedances for transient analysis," *IEEE Transactions on Power Delivery*, vol. 19, no. 3, pp. 1238–1244, 2004.

[29] Y. Baba and M. Ishii, "Numerical electromagnetic field analysis of lightning current in tall structures," *IEEE Transactions on Power Delivery*, vol. 16, no. 2, pp. 324–328, 2001.

[30] B. Kordi, R. Moini, W. Janischewskyj, A. M. Hussein, V. O. Shostak, and V. A. Rakov, "Application of the antenna theory model to a tall tower struck by lightning," *Journal of Geophysical Research: Atmospheres*, vol. 108, no. D17, 2003.

[31] R. Harrington, *Field computation by Moment Methods*. New York: IEEE & Wiley, 1993.

[32] H. Karami, F. Rachidi, and M. Rubinstein, "On practical implementation of electromagnetic models of lightning return-strokes," *Atmosphere*, vol. 7, no. 10, 2016.

[33] M. Nazari, R. Moini, S. Fortin, F. P. Dawalibi, and F. Rachidi, "Impact of frequency-dependent soil models on grounding system performance for direct and indirect lightning strikes," *IEEE Transactions on Electromagnetic Compatibility*, vol. 63, no. 1, pp. 134–144, 2021.

[34] E. Petrache, F. Rachidi, D. Pavanello, W. Janischewskyj, A. M. Hussein, M. Rubinstein, V. Shostak, W. A. Chisholm, and J. S. Chang, "Lightning strikes to elevated structures: influence grounding conditions on currents and electromagnetic fields," in *2005 International Symposium on Electromagnetic Compatibility, 2005. EMC 2005.*, vol. 2, 2005, pp. 377–381 Vol. 2.

[35] L. Zhang, S. Fang, G. Wang, T. Zhao, and L. Zou, "Studies on an electromagnetic transient model of offshore wind turbines and lightning transient overvoltage considering lightning channel wave impedance," *Energies*, vol. 10, no. 12, 2017.

[36] N. Malcolm and R. K. Aggarwal, "Transient overvoltage study of an island wind farm," in *2012 47th International Universities Power Engineering Conference (UPEC)*, 2012, pp. 1–6.

[37] N. Malcolm and R. Aggarwal, "Analysis of transient overvoltage phenomena due to direct lightning strikes on wind turbine blade," in *2014 IEEE PES General Meeting | Conference Exposition*, 2014, pp. 1–5.

[38] D. Romero, J. Montanyà, and A. Candela, "Behaviour of the wind-turbines under lightning strikes including nonlinear grounding system," in *Proceeding International conference on Renewable Energy and Power Quality (ICREPQ'04)*, 2004.

[39] R. Moini, B. Kordi, G. Z. Rafi, and V. A. Rakov, "A new lightning return stroke model based on antenna theory," *Journal of Geophysical Research: Atmospheres*, vol. 105, no. D24, pp. 29 693–29 702, 2000.

[40] F. Gatta, A. Geri, S. Lauria, and M. Maccioni, "Generalized pi-circuit tower grounding model for direct lightning response simulation," *Electric Power Systems Research*, vol. 116, pp. 330–337, 2014.

[41] J. C. Willett, J. C. Bailey, V. P. Idone, A. Eybert-Berard, and L. Barret, "Submicrosecond intercomparison of radiation fields and currents in triggered lightning return strokes based on the transmission-line model," *Journal of Geophysical Research: Atmospheres*, vol. 94, no. D11, pp. 13 275–13 286, 1989. [Online]. Available: https://agupubs.onlinelibrary.wiley.com/doi/abs/10.1029/JD094iD11p13275

[42] S. Visacro and A. Soares, "HEM: a model for simulation of lightning-related engineering problems," *IEEE Transactions on Power Delivery*, vol. 20, no. 2, pp. 1206–1208, 2005.

[43] R. Torchio, "A volume PEEC formulation based on the cell method for electromagnetic problems from low to high frequency," *IEEE Transactions on Antennas and Propagation*, vol. 67, pp. 7452–7465, 2019.

[44] J. Cao, Y. Ding, Y. P. Du, B. Li, R. Qi, Y. Zhang, and Z. Li, "Lightning surge analysis of transmission line towers with a hybrid PEEC-FDTD method," *IEEE Transactions on Power Delivery*, pp. 1–1, 2021.

[45] R. Torchio, D. Voltolina, P. Bettini, F. Moro, and P. Alotto, "Marching on-in-time unstructured PEEC method for electrically large structures with conductive, dielectric, and magnetic media," *Electronics*, vol. 9, no. 2, 2020.

[46] C. Gianfagna, L. Lombardi, and G. Antonini, "Marching-on-in-time solution of delayed PEEC models of conductive and dielectric objects," *IET Microwaves, Antennas & Propagation*, vol. 13, no. 1, pp. 42–47, 2019.

[47] V. A. Rakov, "Lightning return stroke speed," *J. Lightning Res*, vol. 1, pp. 80–89, 2007.

[48] C. Nucci, C. Mazzetti, F. Rachidi, and M. Ianoz, "On lightning return stroke models for LEMP calculations," in *19th International Conference on Lightning Protection, Graz*, 1988.

[49] C. Nucci and F. Rachidi, "Experimental validation of a modification to the transmission line model for LEMP calculation," in *8th Symposium and Technical Exhibition on Electromagnetic Compatibility, Zurich*, 1989.

[50] H. Heidler, "Analytische blitzstromfunktion zur lemp-berechnung," *18th ICLP, Munich, Germany, 1985*, 1985.

[51] S. Guerrieri, C. Nucci, F. Rachidi, and M. Rubinstein, "On the influence of elevated strike objects on directly measured and indirectly estimated lightning currents," *IEEE Transactions on Power Delivery*, vol. 13, no. 4, pp. 1543–1555, 1998.

[52] M. Magdowski, S. Kochetov, and M. Leone, "Modeling the skin effect in the time domain for the simulation of circuit interconnects," in *2008 International Symposium on Electromagnetic Compatibility - EMC Europe*, 2008, pp. 1–6.

[53] A. Shoory, F. Vega, P. Yutthagowith, F. Rachidi, M. Rubinstein, Y. Baba, V. A. Rakov, K. Sheshyekani, and A. Ametani, "On the mechanism of current pulse propagation along conical structures: Application to tall towers struck by lightning," *IEEE Transactions on Electromagnetic Compatibility*, vol. 54, no. 2, pp. 332–342, 2012.

[54] W. Janischewskyj, A. M. Hussein, and V. Shostak, "Propagation of lightning current within the CN tower," in *in Proc. Int. CIGRE Colloq. Insulation Coordination, Toronto, Canada*, vol. 10, no. 33-2, September 1997.

[55] J. Bermudez, F. Rachidi, M. Rubinstein, W. Janischewskyj, V. Shostak, D. Pavanello, J. S. Chang, A. Hussein, C. Nucci, and M. Paolone, "Far-field-current relationship based on the TL model for lightning return strokes to elevated strike objects," *IEEE Transactions on Electromagnetic Compatibility*, vol. 47, no. 1, pp. 146–159, 2005.

[56] L. Feng, L. Lombardi, G. Antonini, and P. Benner, "Stable macromodels for delayed PEEC models with error estimation," in *2021 International Applied Computational Electromagnetics Society Symposium (ACES)*, 2021, pp. 1–4.